Acta Mech 197, 97–117 (2008)
DOI 10.1007/s00707-007-0491-3
Printed in The Netherlands

Acta Mechanica

Vibration analysis of solid ellipsoids and hollow ellipsoidal shells of revolution with variable thickness from a three-dimensional theory

J.-H. Kang[1], **A. W. Leissa**[2]

[1] Department of Architectural Engineering, Chung-Ang University, Seoul, South Korea
[2] Colorado State University, Fort Collins, CO, USA

Received 27 January 2007; Accepted 14 June 2007; Published online 19 October 2007
© Springer-Verlag 2007

Summary. A three-dimensional (3D) method of analysis is presented for determining the free vibration frequencies and mode shapes of complete ellipsoidal shells of revolution with variable thickness and solid ellipsoids. Unlike conventional shell theories, which are mathematically two-dimensional (2D), the present method is based upon the 3D dynamic equations of elasticity. Displacement components u_r, u_θ, and u_z in the radial, circumferential, and axial directions, respectively, are taken to be periodic in θ and in time, and algebraic polynomials in the r and z directions. Potential (strain) and kinetic energies of the ellipsoidal shells of revolution and solid ellipsoids are formulated, and the Ritz method is used to solve the eigenvalue problem, thus yielding upper bound values of the frequencies by minimizing the frequencies. As the degree of the polynomials is increased, frequencies converge to the exact values. Convergence to three or four-digit exactness is demonstrated for the first five frequencies of the ellipsoidal shells of revolution. Numerical results are presented for a variety of ellipsoidal shells with variable thickness. Frequencies for five solid ellipsoids of different axis ratios are also given. Spherical shells and solid spheres are special cases which are included. Comparisons are also made between the frequencies from the present 3D Ritz method, a 2D Ritz method, and a 3D finite element method. The multiple degeneracies (two or more modes having the same frequency) of spherical bodies are examined by analyzing some almost-spherical ellipsoids.

1 Introduction

A vast published literature exists for free vibrations of shells. The monograph of Leissa [1] summarized approximately 1000 relevant publications world-wide through the 1960s. Almost all of these dealt with shells of revolution (e.g., circular cylindrical, conical, spherical). Among them only eighteen references considered ellipsoidal shells. Some additional investigations of dynamic characteristics of ellipsoidal shells have also been uncovered [2]–[14]. However, these studies were almost all based upon **thin** shell theory, which is mathematically **two-dimensional** (2D). That is, for thin shells one assumes the Kirchhoff hypothesis that normals to the shell middle surface remain normal to it during deformations (vibratory, in this case), and unstretched in length. This yields an

Correspondence: Jae-Hoon Kang, Department of Architectural Engineering, Chung-Ang University, 221 Heuksuk-Dong, Dongjak-Ku, 156-756 Seoul, South Korea
e-mail: jhkang@cau.ac.kr

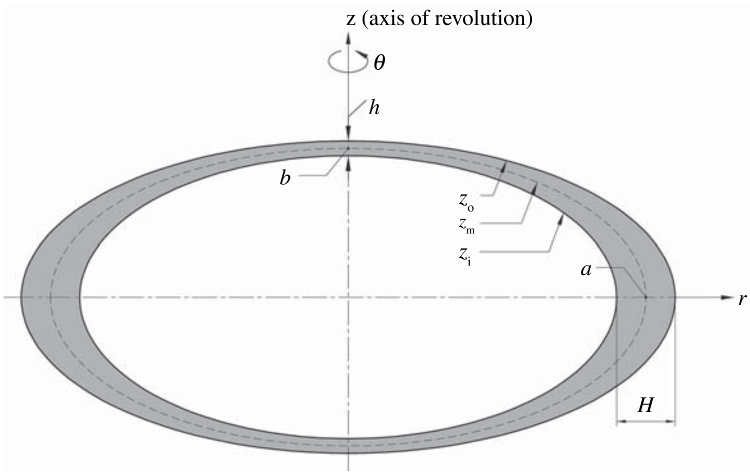

Fig. 1. A cross-section of an ellipsoidal shell of revolution and the cylindrical coordinate system (r, z, θ)

eighth order set of partial differential equations of motion to be solved. For ellipsoidal shells they involve variable coefficients, making them quite difficult to solve.

Even so, conventional shell theory is only applicable to **thin** shells. A higher order shell theory could be used which considers the effects of shear deformation and rotary inertia, and would be useful for the low frequency modes of moderately thick shells [6]. Such a theory would also be 2D. But for ellipsoidal shells the resulting equations would be very complicated.

Recently natural frequencies for the ellipsoidal shells were obtained based upon a 3D theory, however they were for solid **hemi**-ellipsoids and **hemi**-ellipsoidal shells of revolution with uniform thickness [15].

In the present work complete ellipsoidal shells of revolution with variable thickness and solid ellipsoids are analyzed by a 3-D approach. Instead of attempting to solve the equations of motion, an energy approach is followed which, as sufficient freedom is given to the three displacement components, yields frequency values as close to the exact ones as desired. To evaluate the energy integrations over the shell volume **exactly** (not numerically), displacements and strains are expressed in terms of the cylindrical coordinates, instead of related 3D shell coordinates which are normal and tangent to the shell midsurface. Natural frequencies are obtained for five solid ellipsoids and fifteen ellipsoidal shells of revolution, some having variable thickness. Spherical shells and solid spheres are special cases which are included. Comparisons are also made between the frequencies from the present 3D Ritz method, a 2D Ritz method, and a 3D finite element method.

2 Method of analysis

A representative cross-section of an ellipsoidal shell of revolution having variable thickness is shown in Fig. 1. The lengths of major and minor axes of the mid-surface (z_m) of the ellipsoidal shell are $2a$ and $2b$, respectively, and so the mid-surface has the equation of $r^2/a^2 + z^2/b^2 = 1$. The cylindrical coordinate system (r, z, θ), also shown in the figure, is used in the analysis, where θ is the circumferential angle. The shell thicknesses at $z = 0$ and $r = 0$ are H and h, respectively. Thus the domain (Λ) of the ellipsoidal shell of revolution is obtained by subtracting the inner portion

$$0 \le r \le a - \frac{H}{2}, \quad -z_i \le z \le z_i, \quad 0 \le \theta \le 2\pi \tag{1}$$

from the outer portion

$$0 \le r \le a + \frac{H}{2}, \quad -z_o \le z \le z_o, \quad 0 \le \theta \le 2\pi, \tag{2}$$

where $z_{i,o}$ are the coordinates of the inner and outer surfaces of the cross-section for $z \ge 0$ in Fig. 1, respectively,

$$z_{i,o} \equiv \left(b \mp \frac{h}{2}\right)\sqrt{1 - \left(\frac{r}{a \mp H/2}\right)^2}. \tag{3}$$

For mathematical convenience, the radial (r) and axial (z) coordinates are made dimensionless as

$$\psi \equiv \frac{r}{a}, \quad \zeta \equiv \frac{z}{b}. \tag{4}$$

Thus the domain (Λ) of the shell in terms of the nondimensional cylindrical coordinates ($\psi,\ \zeta,\ \theta$) is given by subtracting the inner portion

$$0 \le \psi \le 1 - H^*/2, \quad -\zeta_i \le \zeta \le \zeta_i, \quad 0 \le \theta \le 2\pi \tag{5}$$

from the outer portion

$$0 \le \psi \le 1 + H^*/2, \quad -\zeta_o \le \zeta \le \zeta_o, \quad 0 \le \theta \le 2\pi, \tag{6}$$

where

$$\zeta_{i,o} \equiv \frac{z_{i,o}}{b} = \left(1 \mp \frac{H^* h^*}{2k}\right)\sqrt{1 - \left(\frac{\psi}{1 \mp H^*/2}\right)^2}, \tag{7}$$

with nondimensional thickness parameters of H^* and h^* and the axis ratio k defined by

$$H^* \equiv \frac{H}{a}, \quad h^* \equiv \frac{h}{H}, \quad k \equiv \frac{b}{a}. \tag{8}$$

In the case of **solid** ellipsoids the domain is given by

$$0 \le \psi \le 1, \quad -\sqrt{1-\psi^2} \le \zeta \le \sqrt{1-\psi^2}, \quad 0 \le \theta \le 2\pi. \tag{9}$$

Utilizing tensor analysis, the three equations of motion in terms of the cylindrical coordinate system (r, z, θ) are found to be [16]

$$\sigma_{rr,r} + \sigma_{rz,z} + \frac{1}{r}(\sigma_{rr} - \sigma_{\theta\theta} + \sigma_{r\theta,\theta}) = \rho \ddot{u}_r, \tag{10a}$$

$$\sigma_{rz,r} + \sigma_{zz,z} + \frac{1}{r}(\sigma_{rz} + \sigma_{z\theta,\theta}) = \rho \ddot{u}_z, \tag{10b}$$

$$\sigma_{r\theta,r} + \sigma_{z\theta,z} + \frac{1}{r}(2\sigma_{r\theta} + \sigma_{\theta\theta,\theta}) = \rho \ddot{u}_\theta, \tag{10c}$$

where the σ_{ij} are the normal ($i = j$) and shear ($i \neq j$) stress components; u_r, u_z, and u_θ are the displacement components in the $r, z,$ and θ directions, respectively; ρ is mass density per unit volume; the commas indicate spatial derivatives; and the dots denote time derivatives.

The well-known relationships between the tensorial stresses (σ_{ij}) and strains (ε_{ij}) of isotropic, linear elasticity are

$$\sigma_{ij} = \lambda\varepsilon\delta_{ij} + 2G\varepsilon_{ij}, \tag{11}$$

where λ and G are the Lamé parameters, expressed in terms of Young's modulus (E) and Poisson's ratio (v) for an isotropic solid as

$$\lambda = \frac{Ev}{(1+v)(1-2v)}, \quad G = \frac{E}{2(1+v)}, \tag{12}$$

$\varepsilon \equiv \varepsilon_{rr} + \varepsilon_{zz} + \varepsilon_{\theta\theta}$ is the trace of the strain tensor, and δ_{ij} is Kronecker's delta.

The 3D tensorial strains (ε_{ij}) are found to be related to the three displacements u_r, u_z and u_θ by [16]

$$\varepsilon_{rr} = u_{r,r}, \quad \varepsilon_{zz} = u_{z,z}, \quad \varepsilon_{\theta\theta} = \frac{u_r + u_{\theta,\theta}}{r}, \tag{13a}$$

$$2\varepsilon_{rz} = u_{r,z} + u_{z,r}, \quad 2\varepsilon_{r\theta} = u_{\theta,r} + \frac{u_{r,\theta} - u_\theta}{r}, \quad 2\varepsilon_{z\theta} = u_{\theta,z} + \frac{u_{z,\theta}}{r}. \tag{13b}$$

Substituting Eqs. (11) and (13) into Eqs. (10), one obtains a set of three second-order partial differential equations in u_r, u_z, and u_θ governing free vibrations. However, in the case of ellipsoidal shells, exact solutions are intractable because of the variable coefficients that appear in many terms. Alternatively, one may approach the problem from an energy perspective.

Because the strains are related to the displacement components by Eqs. (13), unacceptable strain singularities may be encountered exactly at $r = 0$ due to the term $1/r$. Since a negligibly small hole does not affect the frequencies [17], such singularities may be avoided by replacing the range for ψ ($\equiv r/a$) in Eqs. (5) and (6), $0 \le \psi \le \psi_{i,o}$, with $10^{-5} \le \psi \le \psi_{i,o}$, and by replacing $0 \le \psi \le 1$ in Eqs. (9) with $10^{-5} \le \psi \le 1$.

During vibratory deformation of the body, its strain (potential) energy (V) is the integral over the domain (Λ):

$$V = \frac{1}{2}\int_\Lambda (\sigma_{rr}\varepsilon_{rr} + \sigma_{zz}\varepsilon_{zz} + \sigma_{\theta\theta}\varepsilon_{\theta\theta} + 2\sigma_{rz}\varepsilon_{rz} + 2\sigma_{r\theta}\varepsilon_{r\theta} + 2\sigma_{z\theta}\varepsilon_{z\theta})\, r\, dr\, dz\, d\theta. \tag{14}$$

Substituting Eqs. (11) and (13) into Eq. (14) results in the strain energy in terms of the three displacements:

$$V = \frac{1}{2}\int_\Lambda [\lambda(\varepsilon_{rr} + \varepsilon_{zz} + \varepsilon_{\theta\theta})^2 + 2G\{\varepsilon_{rr}^2 + \varepsilon_{zz}^2 + \varepsilon_{\theta\theta}^2 + 2(\varepsilon_{rz}^2 + \varepsilon_{z\theta}^2 + \varepsilon_{r\theta}^2)\}]\, r\, dr\, dz\, d\theta, \tag{15}$$

where the tensorial strains ε_{ij} are expressed in terms of the three displacements by Eqs. (13).

The kinetic energy (T) is simply

$$T = \frac{1}{2}\int_\Lambda \rho\,(\dot{u}_r^2 + \dot{u}_z^2 + \dot{u}_\theta^2)\, r dr\, dz\, d\theta\,. \tag{16}$$

For the free, undamped vibration the time (t) response of the three displacements is sinusoidal and, moreover, the circular symmetry of the body of revolution allows the displacements to be expressed by

$$u_r(\psi, \zeta, \theta, t) = U_r(\psi, \zeta)\cos n\theta\, \sin(\omega t + \alpha), \tag{17.1}$$

$$u_z(\psi, \zeta, \theta, t) = U_z(\psi, \zeta)\cos n\theta\, \sin(\omega t + \alpha), \tag{17.2}$$

$$u_\theta(\psi, \zeta, \theta, t) = U_\theta(\psi, \zeta)\sin n\theta\, \sin(\omega t + \alpha), \tag{17.3}$$

where U_r, U_z, and U_θ are displacement functions of ψ and ζ, ω is a natural frequency, and α is an arbitrary phase angle determined by the initial conditions. The circumferential wave number is taken to be an integer (n = 0, 1, 2, . . ., ∞), to ensure periodicity in θ. That the variables separable form of Eqs. (17) does apply may be verified by substituting the displacements into the 3D equations of motion [18]. Then Eqs. (17) account for all free vibration modes except for the torsional ones. The torsional modes arise from an alternative set of solutions which are the same as Eqs. (17), except that cos$n\theta$ and sin$n\theta$ are interchanged. For $n \geq 1$, this set duplicates the solutions of Eqs. (17), with the symmetry axes of the mode shapes being rotated. But for n = 0 the alternative set reduces to $u_r = u_z = 0$, $u_\theta = U_\theta^*(\psi, \zeta)\sin(\omega t + \alpha)$, which corresponds to the torsional modes. The displacements uncouple by circumferential wave number (n), leaving only coupling in r (or ψ) and z (or ζ).

The Ritz method uses the maximum potential (strain) energy ($V_{\max}$) and the maximum kinetic energy ($T_{\max}$) functionals in a cycle of vibratory motion. The functionals for the shell are obtained by setting $\sin^2(\omega t + \alpha)$ and $\cos^2(\omega t + \alpha)$ equal to unity in Eqs. (15) and (16) after the displacements (17) are substituted, and by using the nondimensional coordinates ψ and ζ, as follows:

$$V_{\max} = \frac{bG}{2}\left[\int_0^{1+H^*/2}\int_{-\zeta_o}^{\zeta_o} I_V\,\psi\,d\zeta d\psi - \int_0^{1-H^*/2}\int_{-\zeta_i}^{\zeta_i} I_V\,\psi\,d\zeta\,d\psi\right], \tag{18}$$

$$T_{\max} = \frac{a^2 b\rho\omega^2}{2}\left[\int_0^{1+H^*/2}\int_{-\zeta_o}^{\zeta_o} I_T\,\psi\,d\zeta d\psi - \int_0^{1-H^*/2}\int_{-\zeta_i}^{\zeta_i} I_T\,\psi\,d\zeta\,d\psi\right], \tag{19}$$

where

$$I_V \equiv \left[\frac{\lambda}{G}(\kappa_1+\kappa_2+\kappa_3)^2 + 2(\kappa_1^2+\kappa_2^2+\kappa_3^2) + \kappa_4^2\right]\Gamma_1 + (\kappa_5^2+\kappa_6^2)\Gamma_2, \tag{20}$$

$$I_T \equiv (U_r^2 + U_z^2)\Gamma_1 + U_\theta^2\Gamma_2, \tag{21}$$

and

$$\kappa_1 \equiv \frac{U_r + nU_\theta}{\psi}, \quad \kappa_2 \equiv U_{r,\psi}, \quad \kappa_3 \equiv \frac{U_{z,\zeta}}{k}, \tag{22.1}$$

$$\kappa_4 \equiv U_{z,\psi} + \frac{U_{r,\zeta}}{k}, \quad \kappa_5 \equiv \frac{nU_z}{\psi} - \frac{U_{\theta,\zeta}}{k}, \quad \kappa_6 \equiv \frac{nU_r + U_\theta}{\psi} - U_{\theta,\psi}, \tag{22.2}$$

and Γ_1 and Γ_2 are constants, defined by

$$\Gamma_1 \equiv \int_0^{2\pi} \cos^2 n\theta\,d\theta = \begin{cases} 2\pi & \text{if } n = 0 \\ \pi & \text{if } n \geq 1 \end{cases}, \tag{23.1}$$

$$\Gamma_2 \equiv \int_0^{2\pi} \sin^2 n\theta\,d\theta = \begin{cases} 0 & \text{if } n = 0 \\ \pi & \text{if } n \geq 1 \end{cases}. \tag{23.2}$$

From Eqs. (12) it is seen that the nondimensional constant λ/G in Eq. (20) involves only ν as follows:

$$\frac{\lambda}{G} = \frac{2\nu}{1-2\nu}. \tag{24}$$

For solid ellipsoids, the maximum energy functionals are given simply by

$$V_{\max} = \frac{bG}{2}\int_0^1 \int_{-\sqrt{1-\psi^2}}^{\sqrt{1-\psi^2}} I_V \, \psi \, d\zeta d\psi, \tag{25}$$

$$T_{\max} = \frac{a^2 b\rho\omega^2}{2}\int_0^1 \int_{-\sqrt{1-\psi^2}}^{\sqrt{1-\psi^2}} I_T \, \psi d\zeta \, d\psi. \tag{26}$$

The displacement functions U_r, U_z, and U_θ in Eqs. (17) are further assumed as algebraic polynomials,

$$U_r(\psi,\zeta) = \sum_{i=0}^{I}\sum_{j=0}^{J} A_{ij}\,\psi^i\zeta^j, \tag{27.1}$$

$$U_z(\psi,\zeta) = \sum_{k=0}^{K}\sum_{l=0}^{L} B_{kl}\,\psi^k\zeta^l, \tag{27.2}$$

$$U_\theta(\psi,\zeta) = \sum_{m=0}^{M}\sum_{n=0}^{N} C_{mn}\,\psi^m\zeta^n, \tag{27.3}$$

and similarly for U_θ^*, where i, j, k, l, m and n are integers; I, J, K, L, M and N are the highest degrees taken in the polynomial terms; A_{ij}, B_{kl} and C_{mn} are arbitrary coefficients to be determined. The algebraic polynomials in Eqs. (27) form function sets which are mathematically complete [19, pp. 266–268]. Thus, the function sets are capable of representing any 3D motion of the shell with increasing accuracy as the indices I, J, …, N are increased. In the limit, as sufficient terms are taken, all internal kinematic constraints vanish, and the functions (27) will approach the exact solution as closely as desired.

The eigenvalue problem is formulated by minimizing the free vibration frequencies with respect to the arbitrary coefficients A_{ij}, B_{kl} and C_{mn}, thereby minimizing the effects of the internal constraints present, when the upper limits (I, J, …, N) become large. This corresponds to the equations [20]:

$$\frac{\partial}{\partial A_{ij}}(V_{\max} - T_{\max}) = 0 \quad (i = 0, 1, 2, \ldots, I; \quad j = 0, 1, 2, \ldots, J), \tag{28.1}$$

$$\frac{\partial}{\partial B_{kl}}(V_{\max} - T_{\max}) = 0 \quad (k = 0, 1, 2, \ldots, K; \quad l = 0, 1, 2, \ldots, L), \tag{28.2}$$

$$\frac{\partial}{\partial C_{mn}}(V_{\max} - T_{\max}) = 0 \quad (m = 0, 1, 2, \ldots, M; \quad n = 0, 1, 2, \ldots, N). \tag{28.3}$$

Equations (28) yield a set of $(I + 1)(J + 1) + (K + 1)(L + 1) + (M + 1)(N + 1)$ linear, homogeneous, algebraic equations in the unknowns A_{ij}, B_{kl} and C_{mn}. The equations can be written in the form

$$(\mathbf{K} - \Omega\,\mathbf{M})\,\mathbf{x} = \mathbf{0}, \tag{29}$$

where $\mathbf{K}$ and $\mathbf{M}$ are stiffness and mass matrices resulting from the maximum strain energy ($V_{\max}$) and the maximum kinetic energy ($T_{\max}$), respectively, and Ω is an eigenvalue of the vibrating system, expressed as the square of non-dimensional frequency, $\Omega \equiv \omega^2\, a^2\rho/G$, and the vector $\mathbf{x}$ takes the form

$$\mathbf{x} = (A_{00}, A_{01}, \ldots, A_{IJ};\; B_{00}, B_{01}, \ldots, B_{KL};\; C_{00}, C_{01}, \ldots, C_{MN})^T. \tag{30}$$

For a nontrivial solution, the determinant of the coefficient matrix is set equal to zero, which yields the frequencies (eigenvalues); that is to say $|\mathbf{K} - \Omega\,\mathbf{M}| = 0$. These frequencies are upper bounds on the exact values. The mode shape (eigenfunction) corresponding to each frequency is obtained, in the usual manner, by substituting each Ω back into the set of algebraic equations, and solving for the ratios of coefficients.

3 Convergence studies

To guarantee the accuracy of frequencies obtained by the procedure described above, it is necessary to conduct some convergence studies to determine the number of terms required in the power series of Eqs. (27). A convergence study is based upon the fact that, if the displacements are expressed as power series, all the frequencies obtained by the Ritz method should converge to their exact values in an upper bound manner. If the results do not converge properly, or converge too slowly, it would be likely that the assumed displacement functions chosen are poor ones, or be missing some functions from a minimal complete set of polynomials.

Tables 1–3 are sample convergence studies for three configurations of ellipsoidal shells (b/a = 1/2, 1, 2). All three configurations have uniform, moderate thickness (h/H = 1, H/a = 1/10). In Table 1 the first five frequencies of *torsional* vibration modes ($n = 0^{\mathrm{T}}$) are investigated. Tables 2 and 3 similarly show frequencies for axisymmetric ($n = 0^{\mathrm{A}}$) and lowest order bending ($n = 1$) modes.

To make the study of convergence less complicated, equal numbers of polynomial terms were taken in both the r (or ψ) coordinate (i.e., $I = K = M$) and z (or ζ) coordinate (i.e., $J = L = N$), although some computational optimization could be obtained for some configurations and some mode shapes by using unequal numbers of polynomial terms.

The symbols ***TZ*** and ***TR*** in the tables indicate the total numbers of polynomial terms used through the axial (z or ζ) and the radial (r or ψ) directions, respectively. Note that the frequency determinant order ***DET*** is related to ***TZ*** and ***TR*** as follows:

$$\boldsymbol{DET} = \begin{cases} \boldsymbol{TZ} \times \boldsymbol{TR} & \text{for torsional modes } (n = 0), \\ 2 \times \boldsymbol{TZ} \times \boldsymbol{TR} & \text{for axisymmetric modes } (n = 0), \\ 3 \times \boldsymbol{TZ} \times \boldsymbol{TR} & \text{for general modes } (n \geq 1). \end{cases} \tag{31}$$

Frequencies in underlined, bold-faced type in Tables 1–3 are the most accurate values (to four significant figures) achieved with the smallest determinant sizes.

Tables 1–3 show the monotonic convergence of all five frequencies as ***TZ*** (= $J + 1$, $L + 1$, and $N + 1$ in Eqs. (27)) are increased, as well as ***TR*** (= $I + 1$, $K + 1$, and $M + 1$ in Eqs. (27)). One sees in Table 1, for example, that the first nondimensional frequency in $\omega a\sqrt{\rho/G}$ for $n = 0^{\mathrm{T}}$ converges to four digits (2.948) when as few as (***TZ***, ***TR***) = (10,4) terms are used, which results in ***DET*** $= 10 \times 4 = 40$. Similarly, four digit convergence of the first frequency (1.195) in Table 2 requires a determinant size of $2 \times (11 \times 6) = 132$.

Comparing Tables 1 and 3, it is important to note that the modes for $n = 1$ require much larger size of ***DET*** compared with the torsional modes ($n = 0^{\mathrm{T}}$). This is primarily because only the circumferential displacement components (u_θ) are involved in the torsional modes, whereas all three components enter into the modes having $n \geq 1$, as seen in Eqs. (31).

4 Numerical results for ellipsoidal shells, and discussion

Tables 4–8 present the nondimensional frequencies in $\omega a\sqrt{\rho/G}$ of ellipsoidal shells of revolution with the axis ratios of b/a = 1/3, 1/2, 1, 2 and 3, respectively. Each table is for three shell

Table 1. Convergence of frequencies in $\omega a\sqrt{\rho/G}$ of an ellipsoidal shell of revolution with b/a = 1/2 and H/a = 1/10 having uniform thickness (h/H = 1) for the five lowest *torsional* modes ($n = 0^{\mathrm{T}}$) for ν = 0.3

TZ [a]	***TR*** [b]	***DET*** [c]	**1**	**2**	**3**	**4**	**5**
4	**2**	**8**	3.668	5.702	8.557	20.75	25.20
	4	**16**	2.984	4.265	5.773	8.010	10.22
	6	**24**	2.981	4.235	5.713	7.147	8.512
	8	**32**	2.981	4.227	5.707	7.031	8.401
	10	**40**	2.981	4.227	5.707	7.029	8.401
5	**2**	**10**	3.668	5.476	8.557	11.70	25.20
	4	**20**	2.984	4.222	5.773	7.094	10.22
	6	**30**	2.981	4.208	5.713	6.966	8.512
	8	**40**	2.981	4.207	5.707	6.946	8.401
6	**2**	**12**	3.302	5.476	8.007	11.70	15.10
	4	**24**	2.957	4.222	5.700	7.094	8.672
	6	**36**	2.950	4.208	5.656	6.966	8.347
	8	**48**	2.950	4.207	5.655	6.946	8.298
7	**2**	**14**	3.302	5.373	8.007	10.44	15.10
	4	**28**	2.957	4.219	5.700	7.021	8.672
	6	**42**	2.950	4.206	5.656	6.940	8.347
	7	**49**	2.950	4.206	5.655	6.938	8.300
8	**2**	**16**	3.136	5.373	7.985	10.44	13.05
	4	**32**	2.950	4.219	5.691	7.021	8.468
	6	**48**	2.948	4.206	5.651	6.940	8.292
	7	**56**	2.948	4.206	5.651	6.938	8.289
	8	**64**	2.948	4.205	5.651	6.937	8.287
9	**2**	**18**	3.136	5.025	7.985	10.41	13.05
	4	**36**	2.950	4.210	5.691	7.014	8.468
	6	**54**	2.948	4.205	5.651	6.937	8.292
	7	**63**	2.948	4.205	5.651	6.936	8.289
	8	**72**	2.948	4.205	5.651	**6.935**	8.287
10	**2**	**20**	3.132	5.025	7.541	10.41	12.87
	4	**40**	**2.948**	4.210	5.669	7.014	8.457
	5	**50**	2.948	**4.205**	5.651	6.946	8.321
	6	**60**	2.948	4.205	5.651	6.937	8.288
	7	**70**	2.948	4.205	**5.650**	6.936	8.286
	8	**80**	2.948	4.205	5.650	6.935	**8.284**
11	**2**	**22**	3.132	4.952	7.541	10.06	12.87
	4	**44**	2.948	4.208	5.669	6.976	8.457
	5	**55**	2.948	4.205	5.651	6.941	8.321
	6	**66**	2.948	4.205	5.651	6.936	8.288
	7	**77**	2.948	4.205	5.650	6.935	8.286

[a] ***TZ*** = Total numbers of polynomial terms used in the z (or ζ) direction
[b] ***TR*** = Total numbers of polynomial terms used in the r (or ψ) direction
[c] ***DET*** = Frequency determinant order

configurations of $(H/a, h/H)$ = (1/30, 1), (1/10, 1/5) and (1/10, 1). That is, in each of the five tables, frequencies are given for the ellipsoidal shells with thin uniform thickness, with variable thickness, and with thick uniform thickness. Poisson's ratio (ν) was taken to be 0.3. Thirty-five frequencies are given for each configuration, which arise from seven circumferential wave numbers ($n = 0^{\mathrm{T}}, 0^{A}$, 1, 2, 3, 4, 5) and the first five modes (s = 1, 2, 3, 4, 5) for each value of n, where the superscripts T and A indicate torsional and axisymmetric modes, respectively. The numbers in parentheses identify the first five frequencies for each configuration. The zero frequencies of rigid body modes are omitted from the tables.

Table 2. Convergence of frequencies in $\omega a\sqrt{\rho/G}$ of a **spherical** shell of revolution with b/a = 1 and H/a = 1/10 having uniform thickness (h/H = 1) for the five lowest **axisymmetric** modes ($n = 0^A$) for ν = 0.3

TZ[a]	***TR***[b]	***DET***[c]	**1**	**2**	**3**	**4**	**5**
5	**2**	**20**	1.238	1.876	2.736	3.622	5.020
	4	**40**	1.205	1.521	1.928	2.734	2.788
	6	**60**	1.205	1.507	1.806	2.483	2.733
	8	**80**	1.205	1.507	1.800	2.468	2.731
	10	**100**	1.205	1.506	1.799	2.466	2.723
6	**2**	**24**	1.218	1.779	2.735	3.129	3.351
	4	**48**	1.197	1.501	1.811	2.309	2.729
	6	**72**	1.196	1.472	1.707	2.067	2.654
	8	**96**	1.196	1.471	1.702	2.036	2.482
	10	**120**	1.196	1.470	1.699	2.014	2.452
7	**2**	**28**	1.215	1.588	2.735	2.918	3.350
	4	**56**	1.196	1.478	1.794	2.226	2.728
	6	**84**	1.196	1.470	1.701	2.014	2.501
	8	**112**	1.196	1.469	1.698	1.995	2.435
	10	**140**	1.196	1.469	1.697	1.992	2.410
8	**2**	**32**	1.211	1.573	2.103	2.736	3.350
	4	**64**	1.196	1.473	1.721	2.167	2.728
	6	**96**	1.195	1.469	1.696	2.000	2.414
	8	**128**	1.195	1.468	1.690	1.982	2.380
	10	**160**	1.195	1.468	1.690	1.980	2.370
9	**2**	**36**	1.210	1.551	2.069	2.735	3.005
	4	**72**	1.196	1.470	1.709	2.053	2.697
	6	**108**	1.195	1.468	1.693	1.989	2.400
	7	**126**	1.195	1.468	1.690	1.983	2.389
	8	**144**	1.195	1.468	1.690	1.978	2.370
	9	**162**	1.195	1.468	1.690	1.977	2.366
	10	**180**	1.195	1.468	1.689	1.977	2.366
	11	**198**	1.195	1.468	1.689	1.976	2.364
10	**2**	**40**	1.210	1.548	1.975	2.735	2.934
	4	**80**	1.196	1.469	1.697	2.030	2.517
	6	**120**	1.195	1.468	1.691	1.984	2.385
	7	**140**	1.195	1.468	1.689	1.978	2.371
	8	**160**	1.195	1.468	1.689	1.976	2.364
	9	**180**	1.195	1.468	1.689	1.976	2.361
	10	**200**	1.195	1.468	1.689	1.976	2.360
11	**2**	**44**	1.209	1.548	1.972	2.650	2.734
	4	**88**	**1.195**	**1.468**	1.693	1.999	2.490
	6	**132**	1.195	1.468	**1.689**	1.980	2.377
	7	**154**	1.195	1.468	1.689	1.976	2.364
	8	**176**	1.195	1.468	1.689	**1.975**	2.361
	9	**198**	1.195	1.468	1.689	1.975	**2.359**

[a] ***TZ*** = Total numbers of polynomial terms used in the z (or ζ) direction
[b] ***TR*** = Total numbers of polynomial terms used in the r (or ψ) direction
[c] ***DET*** = Frequency determinant order

It is interesting to note in Tables 4 and 5 that, when $b/a < 1$, the first two frequencies are for axisymmetric modes ($n = 0^A$). This is also true for the spherical (b/a = 1) shells of uniform thickness in Table 6, but not for the variable thickness (h/H = 1/5) case. Tables 7 and 8 show that for $b/a > 1$ the fundamental frequency is for a mode having two circumferential waves in it (n = 2). The torsional frequencies ($n = 0^T$) are all for higher modes.

Table 3. Convergence of frequencies in $\omega a\sqrt{\rho/G}$ of an ellipsoidal shell of revolution with b/a = 2 and H/a = 1/10 having uniform thickness (h/H = 1) for the five lowest bending modes (n = 1) for ν = 0.3

TZ[a]	***TR***[b]	***DET***[c]	**1**	**2**	**3**	**4**	**5**
4	**2**	**24**	1.101	1.213	2.053	2.425	2.769
	4	**48**	1.031	1.130	1.727	1.784	2.326
	6	**72**	1.022	1.126	1.692	1.743	2.235
	8	**96**	1.022	1.126	1.689	1.741	2.232
	10	**120**	1.022	1.126	1.689	1.741	2.230
5	**2**	**30**	1.023	1.142	1.965	2.034	2.707
	4	**60**	0.9902	1.123	1.561	1.747	2.135
	6	**90**	0.9892	1.122	1.546	1.717	1.996
	8	**120**	0.9892	1.122	1.542	1.716	1.947
	10	**150**	0.9892	1.122	1.541	1.716	1.937
6	**2**	**36**	0.9981	1.122	1.616	1.841	2.706
	4	**72**	0.9872	1.115	1.528	1.545	2.028
	6	**108**	0.9868	1.114	1.514	1.519	1.917
	8	**144**	0.9868	1.114	1.507	1.510	1.860
	10	**180**	0.9868	1.114	1.506	1.508	1.846
7	**2**	**42**	0.9905	1.116	1.562	1.658	2.149
	4	**84**	0.9870	**1.114**	1.511	1.516	1.875
	6	**126**	0.9867	1.114	1.497	1.502	1.790
	8	**168**	0.9867	1.114	1.496	1.500	1.781
8	**2**	**48**	0.9887	1.115	1.522	1.582	2.115
	4	**96**	0.9867	1.114	1.497	1.506	1.806
	6	**144**	**0.9866**	1.114	1.492	1.496	1.756
	7	**168**	0.9866	1.114	1.491	1.494	1.751
	8	**192**	0.9866	1.114	1.491	1.494	1.748
9	**2**	**54**	0.9884	1.115	1.513	1.519	2.054
	4	**108**	0.9867	1.114	1.495	1.495	1.782
	6	**162**	0.9866	1.114	1.492	**1.493**	1.751
	7	**189**	0.9866	1.114	1.491	1.493	1.744
	8	**216**	0.9866	1.114	1.491	1.493	1.741
	9	**243**	0.9866	1.114	1.491	1.493	1.741
10	**2**	**60**	0.9883	1.115	1.500	1.513	1.831
	4	**120**	0.9867	1.114	**1.491**	1.495	1.751
	6	**180**	0.9866	1.114	1.491	1.493	1.740
	7	**210**	0.9866	1.114	1.491	1.493	1.739
	8	**240**	0.9866	1.114	1.491	1.493	**1.738**

[a] ***TZ*** = Total numbers of polynomial terms used in the z (or ζ) direction
[b] ***TR*** = Total numbers of polynomial terms used in the r (or ψ) direction
[c] ***DET*** = Frequency determinant order

The spherical shells of Table 6 are particularly interesting in the two cases of uniform thickness (h/H = 1), because of the degeneracies (multiple mode shapes having the same frequencies) present in such cases. Thus, as the table shows, the fundamental frequency then appears for $n = 0^A$, 1 and 2 modes, all three of them. They are all the same mode shape, but looked at from three different directions. Interestingly, further multiple degeneracies are observed in Table 6 as, for example, $\omega R\sqrt{\rho/G}$ = 1.591, which appears for the fourth mode of $n = 0^A$, 1 and 2 when H/a = 1/30, but for the third mode of n = 3, second mode of n = 4, and first mode of n = 5. The degeneracies for spherical shells, as well as solid spheres, will be discussed further in Sect. 7.

Table 4. Frequencies in $\omega a\sqrt{\rho/G}$ of completely free, ellipsoidal shells of revolution with b/a = 1/3 for ν = 0.3

n	*s*	$(H/a,\ h/H)$		
		$(1/30, 1)$	$(1/10, 1/5)$	$(1/10, 1)$
[a]**0**$^{\mathbf{T}}$	**1**	3.302	4.133	3.310
	2	4.527	4.893	4.519
	3	6.243	6.716	6.254
	4	7.508	7.756	7.496
	5	9.093	9.411	9.103
[b]**0**$^{\mathbf{A}}$	**1**	**0.5173(1)**[c]	**0.6792(1)**	**0.6305(1)**
	2	**0.6437(2)**	**0.7031(2)**	**0.9734(2)**
	3	**0.8087(5)**	**0.9088(5)**	1.628
	4	1.028	1.052	2.262
	5	1.342	1.438	3.245
1	**1**	**0.6853(3)**	**0.7735(3)**	**1.029(3)**
	2	**0.7660(4)**	**0.8007(4)**	**1.068(5)**
	3	1.048	1.151	1.644
	4	1.109	1.169	2.346
	5	1.379	1.476	2.539
2	**1**	0.8890	0.9163	**1.059(4)**
	2	0.8901	0.9582	1.530
	3	1.094	1.046	1.966
	4	1.344	1.461	2.122
	5	1.654	1.510	2.574
3	**1**	1.121	1.204	1.616
	2	1.155	1.206	2.109
	3	1.498	1.546	2.781
	4	1.679	1.847	3.143
	5	2.074	2.104	3.600
4	**1**	1.379	1.504	2.194
	2	1.422	1.511	2.747
	3	1.891	2.006	3.607
	4	2.047	2.278	3.969
	5	2.524	2.683	4.630
5	**1**	1.663	1.853	2.818
	2	1.710	1.870	3.433
	3	2.285	2.487	4.463
	4	2.443	2.761	4.707
	5	3.000	3.283	5.656

[a] T = Torsional mode
[b] A = Axisymmetric mode
[c] Numbers in parentheses identify frequency sequence

5 Comparisons with results from 2D shell theory

Jones-Oliveira [9] and Chen and Ginsberg [10] investigated the axisymmetric free vibration properties of thin ellipsoidal shells using the method of assumed modes (which is equivalent to the Rayleigh-Ritz method) based upon the 2D classical linear shell theory including bending effects. The former [9] (2DRL) employed a series of prolate spheroidal angular functions and their derivatives in the displacements. However, because of the difficulty in evaluating those functions, the series were converted to Legendre basis functions. The basis functions the latter [10] (2DRT) used were trigonometric.

Table 5. Frequencies in $\omega a\sqrt{\rho/G}$ of completely free, ellipsoidal shells of revolution with b/a = 1/2 for ν = 0.3

n	*s*	(H/a, h/H)		
		(1/30, 1)	(1/10, 1/5)	(1/10, 1)
[a]**0**^{T}	**1**	2.950	3.669	2.948
	2	4.212	4.678	4.205
	3	5.656	6.052	5.650
	4	6.946	7.247	6.935
	5	8.295	8.562	8.284
[b]**0**^{A}	**1**	**0.7612(1)**[c]	**0.9872(1)**	**0.8239(1)**
	2	**0.8854(2)**	**1.005(2)**	**1.125(2)**
	3	**1.020(5)**	**1.136(5)**	1.618
	4	1.194	1.289	2.234
	5	1.428	1.579	3.036
1	**1**	**0.9458(3)**	**1.055(3)**	**1.146(3)**
	2	**0.9873(4)**	**1.073(4)**	**1.177(4)**
	3	1.186	1.306	1.635
	4	1.222	1.352	2.238
	5	1.451	1.594	2.435
2	**1**	1.146	1.205	**1.309(5)**
	2	1.150	1.211	1.624
	3	1.322	1.301	1.877
	4	1.482	1.331	2.028
	5	1.727	1.597	2.361
3	**1**	1.376	1.471	1.845
	2	1.392	1.472	2.155
	3	1.714	1.815	2.686
	4	1.781	1.992	2.831
	5	2.098	2.135	3.348
4	**1**	1.623	1.785	2.376
	2	1.646	1.793	2.739
	3	2.059	2.249	3.299
	4	2.110	2.458	3.607
	5	2.493	2.745	4.396
5	**1**	1.891	2.161	2.947
	2	1.920	2.181	3.350
	3	2.394	2.732	3.859
	4	2.467	2.948	4.420
	5	2.915	3.314	5.439

[a] T = Torsional mode
[b] A = Axisymmetric mode
[c] Numbers in parentheses identify frequency sequence

Comparisons are made between the frequencies from the present 3D Ritz method (3DR) and two 2D Ritz methods [9], [10] in Table 9 for the first five nondimensional axisymmetric ($n = 0^A$) frequencies in $\rho\omega^2 a^2(1-\nu^2)/E$ of ellipsoidal shells of revolution with uniform thickness (h/H =1) for ν = 0.3.

Table 9 shows for b/a = 1.00504 and 1.4142 that all the five frequencies from 3DR are equal or smaller than ones from the 2D shell analysis methods [9], [10] with an exception of the lowest axisymmetric frequencies ($n = 0^A$) for b/a = 1.4142. However, for b/a = 10.03746 all the five frequencies from 2DRT [10] are smaller than ones from the other two methods (3DR and 2DRL [9]).

Table 6. Frequencies in $\omega a\sqrt{\rho/G}$ of completely free, spherical shells of revolution with $b/a = 1$ for $\nu = 0.3$

n	*s*	(*H*/*a*, *h*/*H*)		
		(1/30, 1)	(1/10, 1/5)	(1/10, 1)
[a]**0**$^{\mathbf{T}}$	**1**	2.000	2.320	**1.996(5)**
	2	3.162	3.515	3.156
	3	4.242	4.581	4.234
	4	5.290	5.600	5.280
	5	6.323	6.602	6.311
[b]**0**$^{\mathbf{A}}$	**1**	**1.186(1)**	**1.387(5)**[c]	**1.195(1)**
	2	**1.410(2)**	1.597	**1.468(2)**
	3	**1.513(3)**	1.723	**1.689(3)**
	4	**1.591(4)**	1.801	**1.975(4)**
	5	**1.675(5)**	1.900	2.359
1	**1**	**1.186(1)**	**1.295(3)**	**1.195(1)**
	2	**1.410(2)**	1.526	**1.468(2)**
	3	**1.513(3)**	1.656	**1.689(3)**
	4	**1.591(4)**	1.763	**1.975(4)**
	5	**1.675(5)**	1.893	**1.996(5)**
2	**1**	**1.186(1)**	**0.9341(1)**	**1.195(1)**
	2	**1.410(2)**	**1.251(2)**	**1.468(2)**
	3	**1.513(3)**	1.551	**1.689(3)**
	4	**1.591(4)**	1.715	**1.975(4)**
	5	**1.675(5)**	1.762	**1.996(5)**
3	**1**	**1.410(2)**	**1.299(4)**	**1.468(2)**
	2	**1.513(3)**	1.507	**1.689(3)**
	3	**1.591(4)**	1.715	**1.975(4)**
	4	**1.675(5)**	1.918	2.359
	5	1.784	2.149	2.840
4	**1**	**1.513(3)**	1.557	**1.689(3)**
	2	**1.591(4)**	1.756	**1.975(4)**
	3	**1.675(5)**	1.980	2.359
	4	1.784	2.230	2.840
	5	1.928	2.518	3.410
5	**1**	1.591(4)	1.845	**1.975(4)**
	2	1.675(5)	2.081	2.359
	3	1.784	2.348	2.840
	4	1.928	2.650	3.410
	5	2.113	2.991	4.067

[a] T = Torsional mode
[b] A = Axisymmetric mode
[c] Numbers in parentheses identify frequency sequence

Lower frequencies are to be expected, because shear deformation and rotary inertia effects are accounted for in a 3D analysis, but not in 2D thin shell analysis.

6 Numerical results for solid ellipsoids, and discussion

Table 10 gives the nondimensional frequencies in $\omega a\sqrt{\rho/G}$ of **solid** ellipsoids with the axis ratios (b/a) of 1/3, 1/2, 1, 2 and 3, which are depicted in Fig. 2. Poisson's ratio (ν) was again taken to be 0.3. It is interesting to note that when $b/a < 1$ the fundamental frequencies are for modes having two ($n = 2$) circumferential waves, unlike the hollow ellipsoidal shells where the fundamental mode is

Table 7. Frequencies in $\omega a\sqrt{\rho/G}$ of completely free, ellipsoidal shells of revolution with $b/a = 2$ for $\nu = 0.3$

n	s	$(H/a,\ h/H)$		
		$(1/30, 1)$	$(1/10, 1/5)$	$(1/10, 1)$
[a]**0**$^{\mathbf{T}}$	**1**	1.144	1.245	1.142
	2	1.890	2.027	1.888
	3	2.598	2.755	2.594
	4	3.288	3.457	3.283
	5	3.969	4.144	3.962
[b]**0**$^{\mathbf{A}}$	**1**	1.169	1.309	1.169
	2	1.548	1.609	1.562
	3	1.634	1.726	1.693
	4	1.700	1.862	1.831
	5	1.785	2.016	1.979
1	**1**	0.9851	1.102	0.9866
	2	1.111	1.152	1.114
	3	1.460	1.525	1.491
	4	1.465	1.569	1.493
	5	1.634	1.777	1.738
2	**1**	**0.4706(1)**[c]	**0.4551(1)**	**0.4934(1)**
	2	0.7912	**0.7428(3)**	**0.8276(3)**
	3	1.070	1.053	1.136
	4	1.278	1.313	1.397
	5	1.432	1.541	1.640
3	**1**	**0.4931(2)**	**0.6035(2)**	**0.6290(2)**
	2	0.7313	**0.8447(4)**	**0.9043(5)**
	3	0.9521	1.095	1.186
	4	1.143	1.340	1.466
	5	1.306	1.580	1.755
4	**1**	**0.5339(3)**	**0.8641(5)**	**0.8938(4)**
	2	**0.7255(5)**	1.079	1.155
	3	0.9132	1.310	1.437
	4	1.090	1.553	1.740
	5	1.256	1.803	2.071
5	**1**	**0.6175(4)**	1.244	1.278
	2	0.7840	1.456	1.549
	3	0.9536	1.687	1.846
	4	1.123	1.936	2.181
	5	1.294	2.197	2.550

[a] T = Torsional mode
[b] A = Axisymmetric mode
[c] Numbers in parentheses identify frequency sequence

axisymmetric ($n = 0^{\mathrm{A}}$). For $b/a > 1$ the fundamental mode for solid ellipsoids is seen to be $n = 1$, whereas for shells it is $n = 2$ (Tables 7 and 8). It is also seen that the axisymmetric modes ($n = 0^{\mathrm{A}}$) are important like the hollow ellipsoidal shells. That is, they are among the lowest frequencies of the solid ellipsoids.

If one holds the semimajor axis length (a) fixed, because it occurs in the nondimensional frequency parameter $\omega a\sqrt{\rho/G}$, increasing b/a then indicates ellipsoids of increasing volume. One usually expects larger bodies to have lower frequencies. This is the case for most of the frequencies in Table 10, but not all of them. Exceptions are seen for the first frequencies having

Table 8. Frequencies in $\omega a\sqrt{\rho/G}$ of completely free, ellipsoidal shells of revolution with $b/a = 3$ for $\nu = 0.3$

n	*s*	$(H\ /\ a,\ h\ /\ H)$		
		$(1/30, 1)$	$(1/10, 1/5)$	$(1/10, 1)$
[a]**0^{T}**	**1**	0.7951	0.8435	0.7943
	2	1.323	1.392	1.321
	3	1.826	1.910	1.824
	4	2.320	2.415	2.317
	5	2.809	2.912	2.806
[b]**0^{A}**	**1**	0.9337	1.035	0.9335
	2	1.453	1.519	1.454
	3	1.604	1.640	1.622
	4	1.653	1.724	1.703
	5	1.717	1.810	1.798
1	**1**	0.5832	**0.6554(5)**	**0.5834(4)**
	2	0.9194	0.9780	0.9212
	3	1.212	1.251	1.219
	4	1.234	1.279	1.237
	5	1.440	1.511	1.468
2	**1**	**0.2369(1)**[c]	**0.2644(1)**	**0.2759(1)**
	2	0.4484	**0.4569(3)**	**0.4895(3)**
	3	0.6792	0.6851	0.7294
	4	0.8937	0.9102	0.9603
	5	1.079	1.118	1.172
3	**1**	**0.2627(2)**	**0.4469(2)**	**0.4592(2)**
	2	**0.4071(4)**	**0.5832(4)**	**0.6161(5)**
	3	0.5685	0.7456	0.7985
	4	0.7315	0.9212	0.9929
	5	0.8871	1.102	1.193
4	**1**	**0.3347(3)**	0.7574	0.7713
	2	**0.4428(5)**	0.8793	0.9185
	3	0.5653	1.019	1.086
	4	0.6946	1.172	1.271
	5	0.8254	1.337	1.471
5	**1**	0.4563	1.167	1.182
	2	0.5473	1.295	1.338
	3	0.6497	1.435	1.512
	4	0.7600	1.589	1.708
	5	0.8757	1.754	1.924

[a] T = Torsional mode
[b] A = Axisymmetric mode
[c] Numbers in parentheses identify frequency sequence

$n = 0^{A}$, 2, 3 and 4 (but not 0^{T} or 1). There, the frequencies first increase, then decrease, with increasing b/a.

Buchanan and Ramirez [21] analyzed the free vibrations of the solid spheres in 3D applying a nine-node Lagrangian finite element and modeling the cross-section of the solid sphere using 50 elements, 231 modes or 694 degrees of freedom. Table 11 shows the comparisons of the first five nondimensional torsional ($n = 0^{T}$) and axisymmetric ($n = 0^{A}$) frequencies in $\omega a\sqrt{\rho/G}$ of a **solid sphere** ($b/a = 1$) from the present 3D Ritz (3DR) method and a 3D finite element method (3DF) [21] for $\nu = 0.3$. It is interesting to note that all the frequencies from the present 3DR are equal to or

Table 9. Comparisons of the first five nondimensional axisymmetric ($n = 0^{A}$) frequencies in $\rho\ \omega^{2}\ a^{2}$ $(1 - \nu^{2})/E$ of ellipsoidal shells of revolution with uniform thickness ($h/H = 1$) from the present 3D Ritz methods (3DR) and two 2D Ritz methods (2DRL [9] and 2DRT [10]) for $\nu = 0.3$

b/a	H/a	Method	**1**	**2**	**3**	**4**	**5**
1.00504	0.0456	3DR	0.494	0.706	0.827	0.945	1.104
		2DRL [9]	0.494	0.706	0.830	0.952	1.116
		2DRT [10]	0.495	0.707	0.831	0.953	1.117
1.4142	0.0388	3DR	0.545	0.825	0.939	1.040	1.157
		2DRL [9]	0.543	0.826	0.944	1.077	1.202
		2DRT [10]	0.544	0.826	0.943	1.047	1.164
10.03746	0.00676912	3DR	0.0376	0.1161	0.2327	0.3829	0.5565
		2DRL [9]	0.0456	0.1286	0.2461	0.4203	0.6185
		2DRT [10]	0.0321	0.1073	0.2225	0.3735	0.5487

Table 10. Frequencies in $\omega a\sqrt{\rho/G}$ of completely free *solid* ellipsoids for $\nu = 0.3$

n	s	b/a				
		1/3	1/2	1	2	3
[a]**0**$^{\mathbf{T}}$	**1**	5.189	4.622	**2.501(1)**	**1.283(2)**	**0.8596(2)**
	2	6.421	5.052	**3.865(4)**	**2.106(5)**	**1.424(5)**
	3	8.460	7.235	5.095	2.878	1.959
	4	8.877	8.177	5.763	3.627	2.481
	5	11.34	8.196	6.266	4.364	2.998
[b]**0**$^{\mathbf{A}}$	**1**	**2.273(2)**[c]	**2.820(3)**	**2.646(2)**	**1.621(3)**	**1.123(4)**
	2	3.842	3.584	**3.530(3)**	2.616	1.910
	3	5.400	5.377	**3.937(5)**	3.323	2.580
	4	7.689	6.183	4.996	3.748	3.095
	5	7.986	7.090	5.007	3.936	3.528
1	**1**	**2.924(5)**	**2.890(4)**	**2.501(1)**	**1.110(1)**	**0.5880(1)**
	2	3.724	3.755	**2.646(2)**	**1.856(4)**	**1.099(3)**
	3	5.947	4.961	**3.530(3)**	2.292	1.620
	4	5.999	5.230	**3.865(4)**	2.601	2.074
	5	6.840	5.917	**3.937(5)**	3.000	2.165
2	**1**	**1.449(1)**	**1.876(1)**	**2.501(1)**	2.454	2.400
	2	**2.780(4)**	**2.761(2)**	**2.646(2)**	2.661	2.548
	3	4.505	4.431	**3.865(4)**	3.159	2.839
	4	5.048	5.002	**3.937(5)**	3.299	3.087
	5	7.329	6.303	5.007	3.773	3.346
3	**1**	**2.542(3)**	**3.134(5)**	**3.865(4)**	3.725	3.673
	2	4.197	4.154	**3.937(5)**	3.955	3.830
	3	6.107	5.932	5.046	4.433	4.109
	4	6.294	6.156	5.095	4.457	4.322
	5	8.547	7.309	6.083	4.976	4.507
4	**1**	3.620	4.324	5.046	4.843	4.792
	2	5.395	5.329	5.095	5.117	4.975
	3	7.489	7.252	6.083	5.549	5.247
	4	7.688	7.321	6.266	5.577	5.457
	5	9.586	8.365	7.087	6.087	5.613

[a] T = Torsional mode
[b] A = Axisymmetric mode
[c] Numbers in parentheses identify frequency sequence

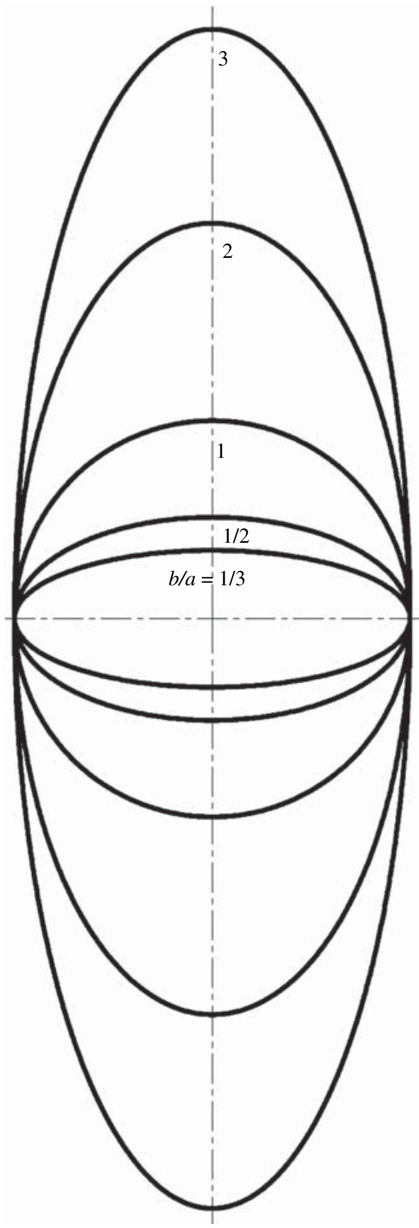

Fig. 2. Cross-sections of solid ellipsoids

less than the ones from 3DF and, in one case, much less (3.530 versus 3.588). The present results are converged to the exact values, to four digits.

7 Viewing degeneracies by means of almost-spherical ellipsoids

It was seen earlier that numerous degeneracies (two or more modes having the same frequency) occur for spherical shells and solid spheres. One can reasonably wonder whether some of the repeated frequencies for $b/a = 1$ (Tables 6 and 10) are correct, or are calculation errors. That they are indeed correct degeneracies can be established by looking at the frequencies of *almost* spherical ellipsoids.

Table 11. Comparisons of the first five nondimensional torsional ($n = 0^T$) and axisymmetric ($n = 0^A$) frequencies in $\omega a\sqrt{\rho/G}$ of a *solid sphere* (b/a = 1) from the present 3D Ritz (3DR) method and a 3D finite element method (3DF) [21] for $\nu = 0.3$

n	Method	1	2	3	4	5
[a]0^T	3DR	2.501	3.865	5.095	5.763	6.266
	3DF	2.501	3.867	5.102	5.765	6.287
[b]0^A	3DR	2.646	3.530	3.937	4.996	5.007
	3DF	2.647	3.588	3.942	4.996	5.009

[a] T = Torsional mode
[b] A = Axisymmetric mode

Table 12. Frequencies in $\omega a\sqrt{\rho/G}$ (including almost degenerate ones) for nearly spherical shells (H/a = 1/10, h/H = 1, $\nu = 0.3$)

n	s	b/a				
		0.97	0.99	1	1.01	1.03
[a]0^T	**1**	2.039	2.010	**1.996(5)**	1.982	1.954
	2	3.213	3.175	3.156	3.137	3.099
	3	4.305	4.257	4.234	4.210	4.164
	4	5.367	5.309	5.280	5.252	5.196
	5	6.412	6.345	6.311	6.278	6.212
[b]0^A	**1**	**1.185(1)**[c]	**1.192(1)**	**1.195(1)**	**1.199(3)**	**1.205(3)**
	2	**1.454(4)**	**1.463(4)**	**1.468(2)**	1.472	1.480
	3	1.684	1.688	**1.689(3)**	1.691	1.695
	4	1.987	1.981	**1.975(4)**	1.975	1.970
	5	2.397	2.379	2.359	2.362	2.345
1	**1**	**1.196(2)**	**1.196(2)**	**1.195(1)**	**1.195(2)**	**1.194(2)**
	2	**1.461(5)**	**1.466(5)**	**1.468(2)**	1.469	1.473
	3	1.688	1.689	**1.689(3)**	1.690	1.691
	4	1.988	1.981	**1.975(4)**	1.975	1.965
	5	2.027	2.006	**1.996(5)**	1.985	1.968
2	**1**	**1.230(3)**	**1.207(3)**	**1.195(1)**	**1.184(1)**	**1.161(1)**
	2	1.483	1.473	**1.468(2)**	**1.462(5)**	**1.451(5)**
	3	1.699	1.693	**1.689(3)**	1.686	1.679
	4	1.993	1.983	**1.975(4)**	1.972	1.962
	5	1.994	1.995	**1.996(5)**	1.997	1.999
3	**1**	1.521	1.485	**1.468(2)**	**1.451(4)**	**1.417(4)**
	2	1.719	1.699	**1.689(3)**	1.679	1.659
	3	2.001	1.985	**1.975(4)**	1.968	1.951
	4	2.397	2.376	2.359	2.354	2.333
	5	2.908	2.877	2.840	2.831	2.816
4	**1**	1.748	1.708	**1.689(3)**	1.670	1.634
	2	2.015	1.989	**1.975(4)**	1.963	1.938
	3	2.398	2.374	2.359	2.349	2.325
	4	2.895	2.862	2.840	2.832	2.805
	5	3.502	3.451	3.410	3.398	3.381
5	**1**	2.033	1.994	**1.975(4)**	1.957	1.922
	2	2.404	2.375	2.359	2.346	2.318
	3	2.891	2.860	2.840	2.830	2.800
	4	3.491	3.453	3.410	3.387	3.358
	5	4.150	4.108	4.067	4.047	4.010

[a] T = Torsional mode
[b] A = Axisymmetric mode
[c] Numbers in parentheses identify frequency sequence

Table 13. Frequencies in $\omega a\sqrt{\rho/G}$ (including almost degenerate ones) for nearly spherical *solid* bodies (v = 0.3)

n	*s*	*b/a*				
		0.97	0.99	1	1.01	1.03
[a]**0^T^**	**1**	**2.573(3)**[c]	**2.525(3)**	**2.501(1)**	**2.478(1)**	**2.433(1)**
	2	3.951	3.893	**3.865(4)**	3.836	3.780
	3	5.196	5.128	5.095	5.061	4.995
	4	5.800	5.775	5.763	5.752	5.731
	5	6.382	6.304	6.266	6.227	6.151
[b]**0^A^**	**1**	2.691	2.661	**2.646(2)**	**2.632(4)**	**2.603(4)**
	2	3.511	3.524	**3.530(3)**	3.536	3.546
	3	4.000	3.958	**3.937(5)**	3.917	3.879
	4	5.025	5.007	4.996	4.972	4.911
	5	5.082	5.032	5.007	4.991	4.958
1	**1**	**2.547(2)**	**2.517(2)**	**2.501(1)**	**2.485(2)**	**2.452(2)**
	2	**2.683(5)**	**2.658(5)**	**2.646(2)**	**2.635(5)**	**2.612(5)**
	3	3.596	3.551	**3.530(3)**	3.510	3.472
	4	3.939	3.889	**3.865(4)**	3.840	3.792
	5	3.995	3.956	**3.937(5)**	3.919	3.884
2	**1**	**2.480(1)**	**2.494(1)**	**2.501(1)**	**2.508(3)**	**2.521(3)**
	2	**2.655(4)**	**2.649(4)**	**2.646(2)**	2.643	2.638
	3	3.904	3.878	**3.865(4)**	3.852	3.827
	4	3.978	3.951	**3.937(5)**	3.924	3.899
	5	5.040	5.018	5.007	4.994	4.962
3	**1**	3.844	3.858	**3.865(4)**	3.871	3.884
	2	3.950	3.942	**3.937(5)**	3.933	3.925
	3	5.088	5.060	5.046	5.032	5.006
	4	5.129	5.106	5.095	5.084	5.062
	5	6.148	6.105	6.083	6.062	6.020
4	**1**	5.060	5.051	5.046	5.041	5.033
	2	5.075	5.088	5.095	5.101	5.112
	3	6.127	6.098	6.083	6.070	6.043
	4	6.298	6.276	6.266	6.256	6.236
	5	7.154	7.109	7.087	7.065	7.023

[a] T = Torsional mode
[b] A = Axisymmetric mode
[c] Numbers in parentheses identify frequency sequence

Table 12 shows the frequencies of spherical (b/a = 1) and almost-spherical (b/a = 0.97, 0.99, 1.01, 1.03) shells having H/a = 1/10 and h/H = 1. The spherical shell frequencies listed are identical to those seen previously in Table 6. The fundamental frequency (1.195) which appears for three degenerate modes ($n = 0^A$, 1, 2) is seen in each case to be a smooth transition in the frequency as b/a is increased from 0.97 to 1.03. That is, if one were to plot $\omega a\sqrt{\rho/G}$ versus b/a, all three curves would cross at b/a = 1. Similarly, the second degenerate frequency (1.468) is the result of four curves crossing at b/a = 1.

Table 13 examines the frequency degeneracies of solid ellipsoids as b/a is increased from 0.97 to 1.03. The frequencies appearing there for b/a = 1 are the same as those in Table 10. Curve crossings at b/a = 1 (solid sphere) similar to those described above are also seen here. Again, the fundamental frequency (2.501) at b/a = 1 involves three degenerate modes; but this time, one of the modes is 0^T, instead of the 0^A mode which was included for the shell. In this case the second degenerate frequency (2.646) is the result of three curves crossing, instead of the four which appeared for the shell.

8 Concluding remarks

Extensive and accurate frequency data determined by the 3D Ritz analysis have been presented for hollow ellipsoidal shells of revolution with variable thickness and also solid ellipsoids. The analysis uses the 3D equations of the theory of elasticity in their general forms for isotropic materials. They are only limited to small strains. No other constraints are placed upon the displacements. This is in significant contrast to the classical 2D thin shell theories, which make very limiting assumptions about the displacement variation through the shell thickness.

The method is straightforward, but it is capable of determining frequencies and mode shapes as close to the exact ones as desired. Therefore, the data in Tables 4–8, 10 and 12–13 may be regarded as benchmark results against which 3D results obtained by other methods, such as finite elements and finite differences, may be compared to determine the accuracy of the latter. Moreover, the frequency determinants required by the present method are at least an order of magnitude smaller than those needed by finite element analyses of comparable accuracy. This was demonstrated extensively in a paper by McGee and Leissa [22]. The Ritz method guarantees upper bound convergence of the frequencies in terms of functions sets that are mathematically complete, such as algebraic polynomials. Some finite element methods can also accomplish this, but at much greater costs, and others cannot.

The method presented could also be extended to circumferentially open ($0 \leq \theta \leq \theta_0$) ellipsoidal shells, instead of circumferentially closed ($0 \leq \theta \leq 2\pi$) ellipsoidal shells of revolution considered in the present work. However, the periodicity in θ would not be present. It would be necessary then to replace the double sums of algebraic polynomials in Eqs. (27) by triple sums, with polynomials in θ being included.

References

[1] Leissa, A. W.: Vibration of shells. Washington DC: US Government Printing Office 1973 (reprinted by The Acoustical Society of America 1993).

[2] Hwang, C.: Extensional vibration of axisymmetrical shells. In: AIAA Annals of Structures and Material Conference, 5th, pp. 227–234. California: Palm Springs 1964.

[3] Bedrosian, B., DiMaggio, F. L.: Transient response of submerged spheroidal shells. Int. J. Solids. Struct. **8**, 111–129 (1972).

[4] Berger, B. S.: The dynamic response of a prolate spheroidal shell submerged in an acoustical medium. J. Appl. Mech. **41**, 925–929 (1974).

[5] Cambou, J. P.: Vibrations libre et axisymetrique des reservoirs quasi-spherique. Acustica **34**, 72–76 (1975).

[6] Burroughs, C. B., Magrab, E. B.: Natural frequencies of prolate spheroidal shells of constant thickness. J. Sound Vibr. **57**, 571–581 (1978).

[7] Ross, C. T. F., Johns, T.: Vibration of submerged hemi-ellipsoidal domes. J. Sound Vibr. **91**, 363–373 (1983).

[8] Popov, A. L., Chernyshev, G. N.: Transition surfaces for short-wave vibrations of an ellipsoidal shell in a fluid. J. Appl. Math. Mech. **49**, 620–624 (1985).

[9] Jones-Oliveira, J. B.: Fluid–solid interaction of a prolate spheroidal shell structures loaded by an acoustic shock wave. PhD Thesis, Massachusetts Institute of Technology 1990.

[10] Chen, P.-T., Ginsberg, J. H.: Modal properties and eigenvalue veering phenomena in the axisymmetric vibration of spheroidal shells. J. Acoust. Soc. Am. **92**, 1499–1508 (1992).

[11] Ross, C. T. F.: Vibration and elastic instability of thin-walled domes under uniform external pressure. Thin-Walled Struct. **26**, 159–177 (1996).

[12] Al-Jumaily, A. M., Najim, F. M.: An approximation to the vibrations of oblate spheroidal shells. J. Sound Vibr. **204**, 561–574 (1997).

[13] Zhang, S. H., Danckert, J., Yuan, S. J., Wang, Z. R., Han, W. J.: Spherical and spheroidal steel structure products made by using integral hydro-bulge forming technology. J. Construct. Steel Res. **46**, 338–339 (paper number 225, full paper on enclosed CD-ROM) (1998).

[14] Chen, P.-T.: Acoustic radiations for submerged elastic structures using natural mode expansions in conjunction with radiation modes approach. J. Sound Vibr. **246**, 245–263 (2001).

[15] Shim, H.-J., Kang, J.-H.: Free vibrations of solid and hollow hemi-ellipsoids revolution from a three-dimensional theory. Int. J. Engng. Sci. **42**, 1793–1815 (2004).

[16] Sokolnikoff, I. S.: Mathematical theory of elasticity, 2nd ed. New York: McGraw-Hill 1956.

[17] Kang, J.-H., Leissa, A. W.: Three-dimensional vibration analysis of solid and hollow hemispheres having varying thickness with and without axial conical holes. J. Vibr. Control. **10**, 199–214 (2004).

[18] Kang, J.-H., Leissa, A. W.: Three-dimensional field equations of motion, and energy functionals for thick shells of revolution with arbitrary curvature and variable thickness. J. Appl. Mech. **68**, 953–954 (2001).

[19] Kantorovich, L. V., Krylov, V. I.: Approximate methods in higher analysis. Groningen, The Netherlands: Noordhoff 1958.

[20] Ritz, W.: Über eine neue Methode zur Lösung gewisser Variationsprobleme der mathematischen Physik. Zeitschrift für die Reine und Angewandte Mathematick **135**, 1–61 (1909).

[21] Buchanan, G. R., Ramirez, G. R.: A note on the vibration of transversely isotropic solid spheres. J. Sound Vibr. **253**, 724–732 (2002).

[22] McGee, O. G., Leissa, A. W.: Three-dimensional free vibrations of thick skewed cantilever plates. J. Sound Vibr. **144**, 305–322 (1991) (errata **149**, 539–542 (1991).